[CANCER RESEARCH 64, 5664–5671, August 15, 2004]

# Decreased Pigment Epithelium-Derived Factor Is Associated with Metastatic Phenotype in Human and Rat Prostate Tumors

**Sofia Halin,[1] Pernilla Wikström,[1] Stina Häggström Rudolfsson,[2] Pär Stattin,[2] Jennifer A. Doll,[3] Susan E. Crawford,[3,4] and Anders Bergh[1]**

*[1]Departments of Medical Biosciences, Pathology and [2]Surgical and Perioperative Sciences, Urology and Andrology, Umeå University, Umeå, Sweden; [3]Department of Pathology, Northwestern University Medical School, Chicago, Illinois; and [4]Robert H. Lurie Comprehensive Cancer Center, Northwestern University Medical School, Chicago, Illinois*

## ABSTRACT

**Pigment epithelium-derived factor, a potent angiogenesis inhibitor in the eye, is also expressed in the prostate. Prostate size and angiogenesis is increased in pigment epithelium-derived factor knockout mice, and pigment epithelium-derived factor is down-regulated in some prostate cancers. To investigate whether pigment epithelium-derived factor expression correlates with tumor progression, we examined 5 Dunning rat prostate sublines with different growth rates, differentiation, androgen dependence, vascular density, and metastatic ability and 26 human prostate cancers of Gleason score 8–10 obtained from patients at transurethral resection selected to represent two groups, with and without metastases at diagnosis. By Western blot, real-time quantitative reverse transcription-PCR, and immunostaining, pigment epithelium-derived factor was detected in highly differentiated, nonmetastatic, androgen-sensitive Dunning tumors and in the anaplastic, androgen insensitive but nonmetastatic Dunning tumors. In contrast, the metastatic Dunning tumor sublines showed very low pigment epithelium-derived factor expression levels. In human cancer tissues, by immunohistochemistry and real-time quantitative reverse transcription-PCR, patients without metastases at diagnosis had higher tumor pigment epithelium-derived factor levels than tumors from patients with metastases at diagnosis. In both the rat model and in the human tumors, the proliferation index and vascular count, as determined by Ki-67 staining and endoglin and/or factor VIII-related antigen staining, inversely correlated with pigment epithelium-derived factor mRNA levels. These observations indicate that loss of pigment epithelium-derived factor expression could be associated with the progression toward a metastatic phenotype in prostate cancer.**

## INTRODUCTION

Disease progression, prognosis, and survival in prostate cancer are related to angiogenesis (1–6). Tumor vascularization correlates with the development of metastatic disease (7). Angiogenesis is regulated by the balance between angiogenesis-inducing and -inhibiting factors. In normal tissues, this balance results in a more or less quiescent vasculature. Pathological angiogenesis requires an increase in stimulating factors, a decrease in inhibiting factors, or both (8, 9). The normal prostate secretes a number of angiogenesis regulating factors (10). A wide variety of proteins including vascular endothelial growth factor (VEGF; Refs. 11–13), transforming growth factor-$\beta$1 (14, 15), fibroblast growth factor-2 (16, 17), and interleukin-8 (18, 19) stimulate angiogenesis in prostate cancer. Angiogenesis inhibitors like thrombospondin-1 are also of importance. Thrombospondin-1 expression is inversely correlated with microvessel density in prostate cancer (20, 21), and thrombospondin-1 treatment inhibits experimental prostate tumor growth (22).

Pigment epithelium-derived factor is one of the most potent inhibitors of angiogenesis known, and it plays a key role in preventing angiogenesis in the healthy eye (23). Pigment epithelium-derived factor blocks the stimulatory activity of multiple inducers of angiogenesis (23), in part by inducing endothelial cell apoptosis (24). In addition to inhibiting angiogenesis, pigment epithelium-derived factor has several other biological effects. It induces neuronal differentiation of retinoblastoma cells (25), is neurotrophic for cerebellar granule cells (26), inhibits microglial growth (27), and is up-regulated during cell cycle phase $G_0$ in young but not senescing cultured fibroblasts (28). The protein belongs to the serine protease inhibitor family but does not inhibit proteases (29, 30). We have shown recently that pigment epithelium-derived factor is expressed in normal rat prostate tissue, in normal human prostate tissue, and in some but not in other human prostate cancer cell lines (31). Pigment epithelium-derived factor protein is up-regulated *in vivo* in both normal rat ventral prostate and human tumor tissue after castration and suppressed *in vitro* by hypoxia (31). In addition, prostate size is markedly increased, the prostate epithelium hyperplastic, and the vascular density increased in pigment epithelium-derived factor knockout mice (31). Pigment epithelium-derived factor expression is often decreased or absent in human prostate tumors compared with adjacent normal tissue (31, 32). These findings indicate that pigment epithelium-derived factor could play an important role in regulating the normal prostate, and its loss in prostate tumors could contribute to tumor progression. Therefore, we examined pigment epithelium-derived factor expression during progression of prostate tumors toward metastatic and hormone refractory disease in a well-characterized model, the Dunning rat adenocarcinoma sublines, as well as in human prostate cancer.

## MATERIALS AND METHODS

**Animals.** Tumor sublines, chosen to represent different prostate tumor grades included the following: Dunning R3327 PAP, slow growing, androgen sensitive, well-differentiated, and nonmetastatic (33); AT-1 and AT-2, fast growing, androgen insensitive, anaplastic, with low to moderate metastatic capacity (34); and AT-3 and MatLyLu, fast growing, androgen insensitive, anaplastic, and highly metastatic (34). Small pieces of tumor or cells were s.c. transplanted or inoculated, respectively, into male Copenhagen x Fisher and Copenhagen rats as described previously (11, 33, 34). When tumors had reached a size of about 1–2 cm in diameter, the animals were sacrificed and the tumors were quickly removed, frozen in liquid nitrogen, and stored in −80°C before RNA or protein extraction. Frozen tumors were postfixated in formalin and paraffin-embedded before immunohistochemistry. All of the animal work was approved by the local ethical committee for animal research.

**Cell Culture.** Cell lines (AT-1, AT-2, AT-3, and MatLyLu) were grown in culture as described previously (34) before RNA or protein extraction. For protein analysis, serum-free conditioned medium was collected as described previously (31). Briefly, cell cultures were grown to approximately 70–80% confluence, rinsed twice with PBS, incubated in serum-free medium for 4 h, and washed. Fresh serum-free medium was added, and cells were incubated at 37°C, 5% $CO_2$. After 48 h, the medium was collected and subjected to centrifugation to remove debris, concentrated, and dialyzed against PBS using Millipore centrifugal filters with a 10 kDa cutoff, according to the manufacturer's description (Millipore Corporation, MA). The BCA Protein Assay (Pierce Chemical Co., Rockford, IL) was used to determine the protein concentration.

Received 3/8/04; revised 6/2/04; accepted 6/11/04.

**Grant support:** Swedish Cancer Society, the University Hospital of Northern Sweden, and the Lions Cancer Research Foundation, Umeå University.

The costs of publication of this article were defrayed in part by the payment of page charges. This article must therefore be hereby marked *advertisement* in accordance with 18 U.S.C. Section 1734 solely to indicate this fact.

**Requests for reprints:** Department of Medical Biosciences, Pathology, Umeå University, S 90187 Umeå, Sweden. E-mail: anders.bergh@medbio.umu.se.

**Human Tissues.** Formalin-fixed, paraffin-embedded specimens from 26 tumors with Gleason score 8–10 (35) were selected from a series of prostate tumors, consecutively diagnosed at transurethral resection at the Central Hospital in Västerås, Sweden, between 1975 and 1983, with complete clinical follow-up (36). Local tumor stage was determined at the time of surgery by digital rectal examination, according to the 1978 Union Internationale Contre le Cancer classification (37), and the presence of metastasis was evaluated by a bone scan. Regional lymph node status was not examined. The tumors were selected to include two groups: (M1) presence of bone metastases at diagnosis and survival ≤5 years ($n = 13$); and (M0) no presence of bone metastases at diagnosis and survival >7 years ($n = 13$). To examine whether there were differences in tumor size between these two groups the volume density of tumor tissue in the transurethral resection specimens was determined using a square-lattice mounted in the eye-piece of a light microscope and counting the number of grip intersections falling on tumor tissue and reference space, as described (5). Serum levels of prostate-specific antigen were not measured, because this series was collected before the prostate specific antigen era. The study was approved by the Institutional Review Board.

**Protein Preparation and Western Blot.** Frozen tumor tissues were homogenized using a Micro Dishmembrator (B.Braun Biotech International GmbH, Melsungen, Germany) at 2000 rpm for 45 s. The homogenized tumors and cell lines were transferred into a lysis buffer containing 0.5% NP40, 0.5% NaDOC, 0.1% SDS, 50 mM Tris-HCl (pH 7.5), 150 mM NaCl, 1 mM EDTA (pH 8.0), 1 mM NaF, and Complete protease inhibitor (Boehringer, Mannheim, Germany). Samples were incubated on ice for 30 min, and supernatants were isolated after 30 min of centrifugation (18,000 rpm; 4°C). The protein concentration was determined as above.

Protein samples were mixed with electrophoresis sample buffer containing 2% SDS and 5% 2-mercaptoethanol and boiled for 10 min. Tumor protein (50 μg) or conditioned medium (10 μg) samples were separated by electrophoresis on a 7.5% SDS-polyacrylamide gel. The fractionated proteins were electroblotted onto a polyvinylidene difluoride membrane (Bio-Rad Laboratories AB, Sundbyberg, Sweden). The membranes were blocked overnight in 5% dry milk, 0.1% Tween 20 in PBS then incubated with primary antibodies, diluted 1:500, for 1 h (23). After washing in 5% dry milk, 0.1% Tween 20, membranes were incubated with peroxidase-conjugated secondary antibodies for 1 h, and proteins were detected using the enhanced chemiluminescence plus detection system (Amersham Biosciences, Uppsala, Sweden). Actin (Sigma, Stockholm, Sweden) or Coomassie-stained gels confirmed equal loading. Molecular size standards (Bio-Rad Laboratories AB) and human pigment epithelium-derived factor (Chemicon International, Hampshire, United Kingdom) were included as controls. Relative pigment epithelium-derived factor expression in conditioned media samples were quantified with densitometry with normalization to an equally loaded Coomassie-stained gel.

**Morphological Analysis.** Human and rodent tumor tissue sections were deparaffinated and rehydrated, according to standard procedures, and washed with PBS. Immunohistochemical staining was performed using primary antibodies against pigment epithelium-derived factor (23), VEGF (Santa Cruz Biotechnology, Santa Cruz, CA; sc-507), Ki-67, endoglin, and factor VIII-related antigen (DAKO Corporation) as described (6, 38, 39). The slides were routinely counterstained with Meyer's hematoxylin solution and mounted. Specificity of the antipigment epithelium-derived factor antibody was examined by preincubation of the antibody with a 10-fold excess (w/w) of a pigment epithelium-derived factor control peptide (Chemicon International). For the rat tumors, the number of Ki-67-labeled tumor cells was counted in 1000 cells/tumor, and the volume density of factor VIII-related antigen-stained blood vessels was determined using a stereological method as described (11). The immunoreactivity of the human tumor sections was evaluated without any knowledge of patient data. Pigment epithelium-derived factor sections were scored by one pathologist, according to an immunoreactive score. The immunoreactive score was determined by multiplying an estimate of the fraction of immunoreactive cells (quantity score, 0–1) with an estimate of the staining intensity (intensity score, 0 = unstained; 1 = weak staining of same intensity as adjacent epithelial cells in nonmalignant glands; and 2 = intense staining, more intense than in adjacent nonmalignant glands). Immunoreactive score could, thus, vary from 0 to 2. Ki-67-positive cells were counted in three hot spot fields, at ×400 magnification, and the percentage of proliferating tumor cells was calculated for each tumor using the analySIS software 3.2 (Soft Imaging System, Münster, Germany). Microvessels were counted at ×200 magnification in three hot spots for each tumor. Two different vascular markers were used on human tissues, because they are known to stain partly different types of blood vessels in prostate cancer. Endoglin stains immature newly formed vessels whereas factor VIII-related antigen stains more mature ones (6). The endoglin antibody does not work in rat tissues. Any positively stained cell was counted; a visible lumen was not required (5, 6). The mean vascular count was used in the statistical analysis.

**Laser Capture Microdissection.** Human tissue samples were cut in 5-μm-thick sections and mounted on HistoGene laser capture microdissection slides (Arcturus, Mountain View, CA). Sections were deparaffinized twice in xylene for 5 min and rehydrated in 100% ethanol, 95% ethanol, 70% ethanol, and RNase-free water for 5 min each, before stained with an laser capture microdissection staining solution (Arcturus) for 20 s. Thereafter, sections were rinsed in RNase-free water, before dehydrated in 70% ethanol, 95% ethanol, 100% ethanol for 30 s, each followed by two changes of xylene for 5 min. Sections were allowed to air-dry before stored in an exicator and microdissected the same day. Cancer epithelial cells were identified by a pathologist and retrieved by laser capture microdissection using the Arcturus PixCell II system (Arcturus). An equal number of selected tumor cells was captured for each patient (1000 shots, laser diameter 15 μm) on the CapSure device (Arcturus) according to the manufacturer's description.

**RNA Preparation and Real-Time Quantitative Reverse Transcription-PCR.** Total RNA from the rat tissues and cell lines were isolated according to the TRIzol method (Invitrogen, Stockholm, Sweden). RNA concentrations were quantified spectrophotometrically at 260 nm (DU 640 Spectrophotometer, Beckman Coulter, Bromma, Sweden). RNA integrity was verified by ethidium bromide staining of 28 S and 18 S rRNA after agarose gel electrophoresis. RNA from microdissected cells was isolated essentially as described previously (40). Briefly, cancer cells adhered to the laser capture microdissection cap were incubated in 40 μl RNA lysis buffer [10 mM Tris-HCL (pH 8.0), 0.1 mM EDTA (pH 8.0), 2% SDS (pH 7.3), and 500 μg/ml Proteinase K (Sigma)] overnight at 60°C, followed by Proteinase K heat inactivation at 95°C for 5 min. RNA was purified by phenol-chloroform extractions followed by a 2-h precipitation at −20°C with an equal volume of isopropanol in the presence of 0.1 volume of 2 M sodium acetate (pH 4.0) and 20 μg of carrier glycogen (Invitrogen). The RNA pellet was washed once in 70% ethanol, dried, and resuspended in 10 μl of RNase-free water.

Total RNA (500 ng) from each rat tumor tissue and cell line or total RNA from 500 microdissected shots of each human sample was reverse transcribed using random hexamers (Applied Biosystems, Sundbyberg, Sweden) and Superscript II reverse transcriptase (Invitrogen) in a 10-μl reaction according to the manufacturer's instructions. All of the cDNA reactions were performed in duplicate. Rat cDNA samples were diluted 1:10, and human samples were diluted 1:2.5 in nuclease-free water.

Quantification of the pigment epithelium-derived factor, VEGF, and glyceraldehyde-3-phosphate dehydrogenase (GAPDH) mRNA levels were performed by real-time reverse transcribed-PCR using the LightCycler SYBR Green I technology (Roche Diagnostics, Bromma, Sweden). Reactions were performed with 2 μl of rat cDNA, 2 or 3 μl of human cDNA, 0.5 μM pigment epithelium-derived factor, VEGF, or GAPDH primers (Table 1), and 3 mM $MgCl_2$, according to the manufacturer's instructions, in a total volume of 20 μl. Negative controls were always run in parallel. Data were analyzed with the LightCycler analysis Software 3.5.3 (Roche Diagnostics). Relative pigment epithelium-derived factor, VEGF, and GAPDH mRNA values were calculated from standard curves obtained by amplification of 5-fold serial dilutions of 125 ng/μl reverse-transcribed total RNA from the rat dorsolateral prostate or by amplification of 2-fold serial dilutions of pooled cDNA from microdissected human prostate tissue. Mean mRNA levels and SE were calculated for each tumor group.

**Statistical Analysis.** The Mann-Whitney *U* test was used for comparison between groups. The Spearman's rho test was used for the correlation studies. A P value $< 0.05$ was considered significant. Statistical analysis was performed using the statistical software SPSS 11.5.

## RESULTS

**Pigment Epithelium-Derived Factor Expression in Dunning Rat Prostate Tumors.** To determine the relationship between pigment epithelium-derived factor expression and tumor progression

Table 1 *Oligonucleotides used as primers in the reverse transcription-PCR reactions*

| Primer name | Nucleotide sequence |
|---|---|
| PEDF-forward rat | 5′-TCT CCT TGG CGT GGC T-3′ (648–663, exon 5 of mouse cDNA, accession no. AF017057) |
| PEDF-reverse rat | 5′-GCC GTA TCG TAA GAT GGC CT-3′ (773–792, exon 6 of mouse cDNA, accession no. AF017057) |
| PEDF-forward human | 5′-CGA AGG CGA AGT CAC CAA GT-3′ (1036–1055, exon 6 of human cDNA, accession no. AF400442) |
| PEDF-reverse human | 5′-GGG TTT GCC TGT GAT CTT GC-3′ (1104–1123, exon 7 of human cDNA, accession no. AF400442) |
| GAPDH-forward | 5′-TGC ACC ACC AAC TGC TTA GC-3′ (514–533, exon 7 of human cDNA, accession no. M33197) |
| GAPDH-reverse | 5′-GGC ATG GAC TGT GGT CAT GAG-3′ (580–600, exon 7–8 of human cDNA, accession no. M33197) |
| VEGF-forward | 5′-GAA GTG GTG AAG TTC ATG GAT GT-3′ (171–193, exon 2–3 of human cDNA, accession no. M32977) |
| VEGF-reverse | 5′-TGG AAG ATG TCC ACC AGG GTC-3′ (224–243, exon 3 of human cDNA, accession no. M32977) |

Abbreviations: PEDF, pigment epithelium-derived factor.

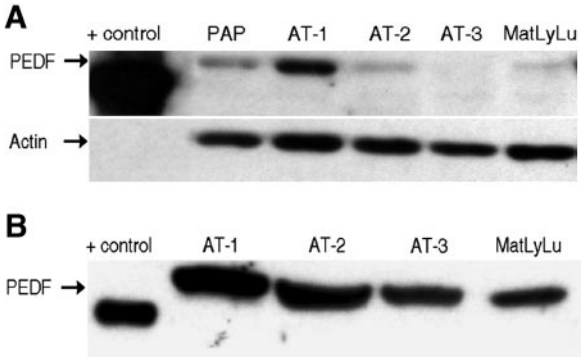


Fig. 1. Pigment epithelium-derived factor (*PEDF*) expression in Dunning rat tumor cells. *A*, Western blot of PEDF in Dunning tumor homogenates by 7.5% SDS-PAGE under reducing conditions. Human PEDF control peptide, 46 kDa, served as a positive control. Actin served as a control for equal loading. *B*, PEDF detected by immunoblot in the conditioned medium from Dunning tumor cell lines grown *in vitro*. Positive control, human PEDF.

toward a metastatic phenotype, we examined pigment epithelium-derived factor protein and mRNA expression levels in the Dunning rat prostate tumor subtypes PAP, AT-1, AT-2, AT-3, and MatLyLu. On Western blots, the pigment epithelium-derived factor antibody recognized a protein with an approximate weight of $M_r$ 50,000, which corresponded to that reported for human pigment epithelium-derived factor (25). Pigment epithelium-derived factor protein was detected in tissue homogenates of the highly differentiated, nonmetastatic, and androgen sensitive PAP tumor and also in the anaplastic, androgen-insensitive but nonmetastatic AT-1 tumor (Fig. 1*A*). In contrast, the anaplastic and highly metastatic sublines, AT-3 and MatLyLu, showed low expression levels of pigment epithelium-derived factor protein (Fig. 1*A*). Whereas PAP is propagated only as an explant, AT-1, AT-2, AT-3, and MatLyLu can be grown in culture; thus, we also compared their *in vitro* expression. This revealed a similar pattern, with relatively higher pigment epithelium-derived factor expression in the AT-1 cell-conditioned medium compared with that from the AT-2, AT-3, and MatLyLu cells (Fig. 1*B*). When these protein levels were quantified by densitometry, the pigment epithelium-derived factor levels in AT-2, AT-3, and MatLyLu were 55%, 81%, and 84% less, respectively, than the level detected in AT-1.

To observe pigment epithelium-derived factor expression in tumor tissue, sections from the Dunning tumors were immunostained with pigment epithelium-derived factor antibody (Fig. 2). In the PAP tumors, a moderate cytoplasmic pigment epithelium-derived factor immunostaining was observed in the epithelial cells. In the AT-1 tumors, intense pigment epithelium-derived factor immunostaining was observed in the tumor epithelial cells adjacent to blood vessels. A similar but less intense pattern was also observed in the AT-2 tumors.

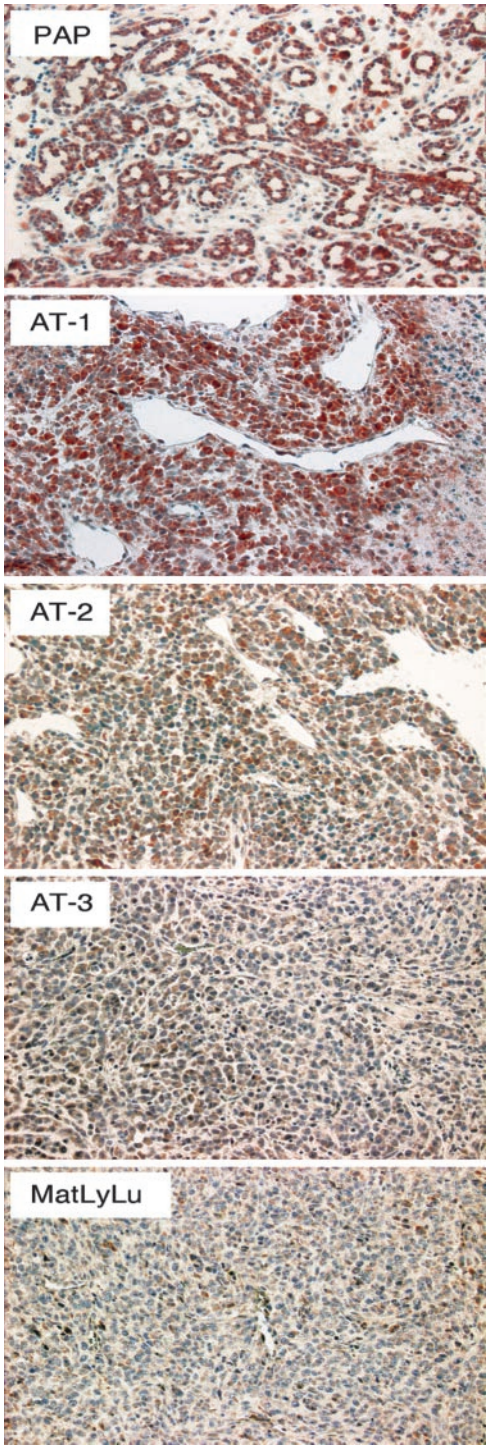


Fig. 2. Pigment epithelium-derived factor (PEDF) immunostaining of Dunning rat tumors. Sections from rat Dunning tumors (PAP, AT-1, AT-2, AT-3 and MatLyLu) immunostained with PEDF antibody, at ×200 magnification. Note the intense perivascular PEDF staining observed in the AT-1 tumor.

A weak, diffuse, or totally absent pigment epithelium-derived factor immunostaining was observed in the epithelial cells in the AT-3 and MatLyLu tumors. As a control, AT-1 tumor sections were stained with pigment epithelium-derived factor antibody preincubated with a pigment epithelium-derived factor peptide. These sections did not demonstrate the intense immunostaining around the blood vessels (data not shown). These data suggest that decreased pigment epithelium-derived factor protein levels may contribute to tumor progression.

To determine whether the pigment epithelium-derived factor mRNA levels were also decreased, we quantified the mRNA levels using real-time quantitative reverse transcription-PCR analysis. All of the Dunning tumor subtypes, grown s.c. and in culture, expressed pigment epithelium-derived factor mRNA. Similar to the protein data, pigment epithelium-derived factor mRNA levels in PAP and AT-1 were significantly higher than in the anaplastic and highly metastatic tumors, AT-3 and MatLyLu (Fig. 3*A*). The relative *in vivo* pigment epithelium-derived factor mRNA expression levels in the different tumor sublines were consistent with the *in vitro* expression levels (data not shown), suggesting that the decreased pigment epithelium-derived factor protein expression may result from decreased mRNA levels.

To additionally examine the differences between the nonmetastasizing AT-1 tumor and the metastasizing MatLyLu tumor, vascular density and epithelial proliferation index were evaluated by factor VIII-related antigen and Ki-67 immunohistochemical staining, respectively. As shown previously (11), the vascular density was significantly higher in the highly metastatic MatLyLu tumor, 5.5 ± 0.5%, compared with the low metastatic AT-1 tumor, 2.4 ± 0.2% (Fig. 3*B*; values are means ± SE; $P < 0.01$). In addition, a significantly higher tumor proliferation index was detected in the MatLyLu tumor, 47.0 ± 3.2%, compared with the AT-1 tumor, 27.8 ± 1.6% (Fig. 3*C*; values are means ± SE; $P < 0.01$). Pigment epithelium-derived factor mRNA levels were inversely correlated to both the vascular count ($r_s = -0.748$; $P < 0.01$) and the proliferation index ($r_s = -0.764$; $P < 0.01$) in these tumors, suggesting that decreased pigment epithelium-derived factor expression could contribute to metastatic spread by increasing angiogenesis and/or the tumor cell proliferation.

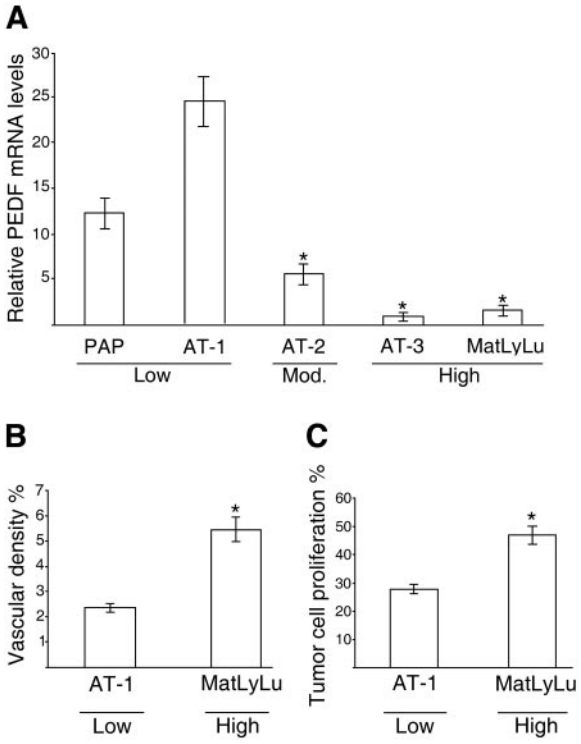


Fig. 3. Pigment epithelium-derived factor (*PEDF*) mRNA, vascular density, and cell proliferation in Dunning tumors. *A*, relative PEDF mRNA levels in rat Dunning tumors quantified with real-time PCR and expressed in relation to the levels in AT-3. Values are expressed as means of 6–10 rats in each group; *bars*, ±SE. *, $P < 0.01$ when the low metastatic tumors (*PAP* and *AT-1*) are compared with the moderately (*AT-2*) and highly metastatic tumors (*AT-3* and *MatLyLu*). *B*, volume density expressed as the percentage of tumor tissue occupied by factor VIII-related antigen stained vessel walls and lumina. Values are means; *bars*, ±SE. *, $P < 0.01$. *C*, tumor cell proliferation expressed as percentage of Ki-67-positive tumor cells. Values are means; *bars*, ±SE. *, $P < 0.01$

Table 2 *Characteristics of patient tumors, Gleason score 8–10*

| | Patient tumor stage* | | |
|---|---|---|---|
| Tumor parameter† | M1 ($n = 13$) | M0 ($n = 13$) | *P* value |
| Proliferation index (%) | 11.8 ± 0.9 | 7.9 ± 1.7 | 0.002 |
| Vascular counts–endoglin | 32.5 ± 2.7 | 21.8 ± 1.0 | 0.0004 |
| Vascular counts–factor VIII-related antigen | 88.1 ± 7.6 | 74.2 ± 6.4 | 0.13 |
| Fraction of transurethral resection specimen composed of tumor (%) | 80.8 ± 5.1 | 62.3 ± 8.0 | 0.07 |
| PEDF immunoreactive score | 1.2 ± 0.1 | 1.7 ± 0.1 | 0.01 |
| Relative PEDF mRNA levels‡ | 1 ± 0.3 | 6.2 ± 1.5 | 0.001 |
| Relative VEGF mRNA levels‡ | 1 ± 0.2 | 1.6 ± 0.4 | 0.15 |

Abbreviations: PEDF, pigment epithelium-derived factor.

* For details on procedures see "Materials and Methods." Values given are means ± SE.

† Stage M1 group had bone metastasis at diagnosis and survival ≤5 years; stage M0 group had no bone metastasis at diagnosis and survival >7 years.

‡ Relative differences between the M1 and M0 groups are expressed as means ± SE when the M1 group is set as one.

**Pigment Epithelium-Derived Factor Expression in Poorly Differentiated Human Prostate Cancer.** We showed recently that pigment epithelium-derived factor is expressed in normal human prostate tissue and that it is often decreased or even absent in human prostate tumors (31). Our present observations in Dunning tumors suggested that decreased pigment epithelium-derived factor expression is associated with an increased metastatic potential. Therefore, it was of interest to determine whether a similar pattern existed in human prostate tumors. To examine this, tissues from patients with poorly differentiated tumors (Gleason score 8–10) were divided into two groups: with and without presence of bone metastases at diagnosis, tumor stage M1 and M0, respectively (Table 2). In both of these groups the tumors were occupying substantial parts of the transurethral resection material, and there was no apparent difference in tumor size between the two groups (Table 2). In these tumors, pigment epithelium-derived factor immunostaining was variable. In some, the cancer cell staining intensity was considerably higher than in adjacent nonmalignant epithelial cells, which showed a very discrete staining, whereas other tumors were largely unstained (Fig. 4*A*). The immunostaining intensity and number of pigment epithelium-derived factor-positive cells were analyzed and combined to generate an immunoreactive score. The immunoreactive score was significantly higher in the less aggressive, poorly differentiated human tumors than in the more aggressive, metastatic ones (Table 2; Fig. 4*A*). To determine whether pigment epithelium-derived factor mRNA levels were also decreased, mRNA was extracted from tumor epithelial cells of microdissected tissue. The pigment epithelium-derived factor mRNA level was significantly higher in patients without metastases compared with patients with metastasis (Table 2). However, no significant correlation between pigment epithelium-derived factor mRNA and immunoreactive score was found.

To evaluate the relationship of pigment epithelium-derived factor expression to other tumor parameters, we immunostained the human tumors using Ki-67, for proliferation index, and using endoglin and factor VIII-related antigen, for vascular density. In the metastatic tumors, the tumor epithelial cell proliferation index and endoglin vascular count were significantly higher than in the less metastatic

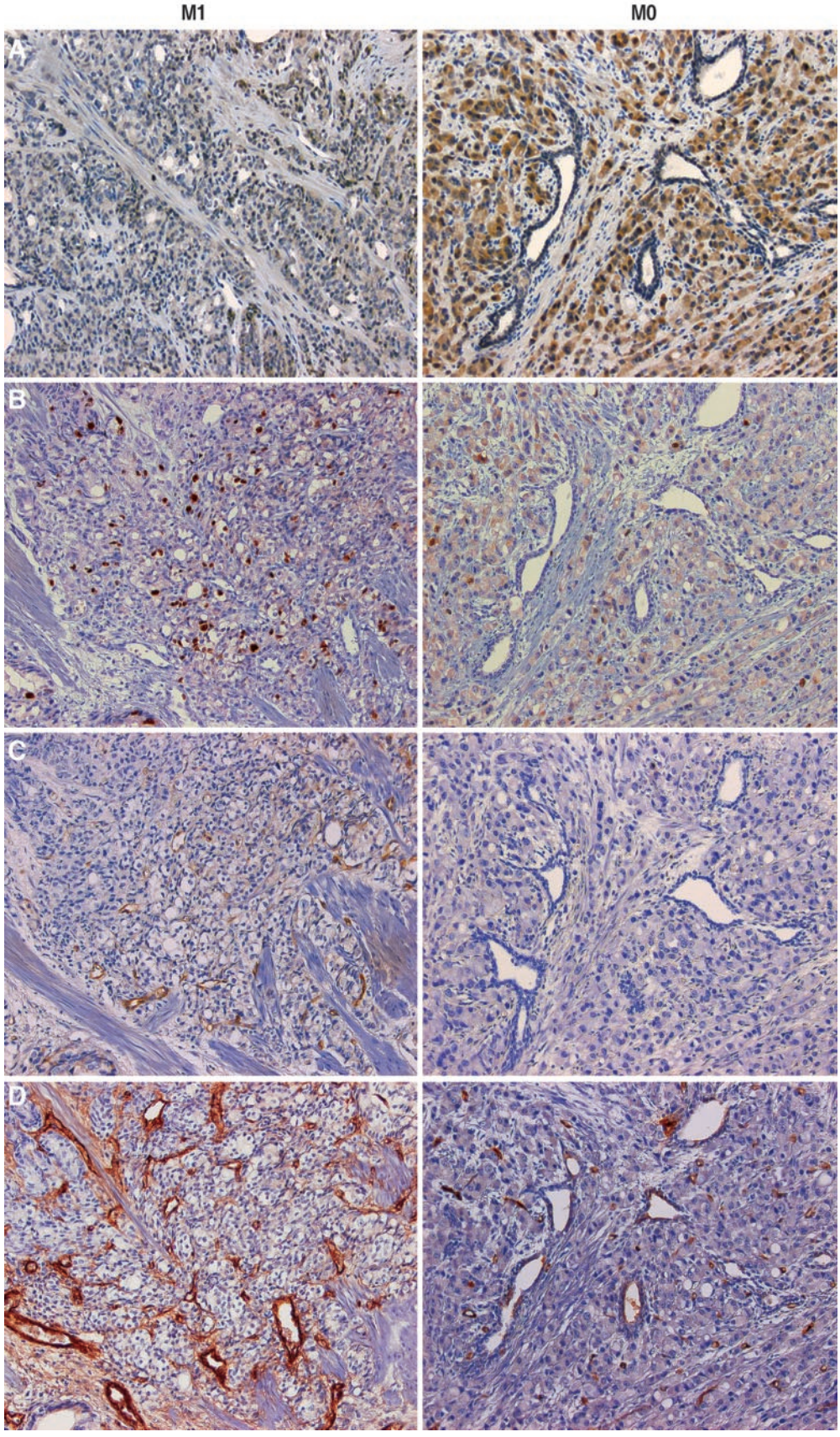


Fig. 4. Immunostaining of human prostate tumors. Transurethral resection sections from prostate cancer patients with the presence of bone metastases at diagnosis (M1) and no presence of bone metastases at diagnosis (M0), immunostained with antibodies against *A*, pigment epithelium-derived factor; *B*, Ki-67; *C*, endoglin; and *D*, factor VIII-related antigen (×200 magnification).

tumors (Table 2; Fig. 4, *B* and *C*). The pigment epithelium-derived factor mRNA levels inversely correlated to both the proliferation index ($r_s = -0.532$; $P < 0.05$) and the endoglin vascular count ($r_s = -0.476$; $P < 0.05$). Vascular density determined by factor VIII-related antigen staining was not significantly different between the two patient groups (Table 2; Fig. 4*D*), and there was no correlation between pigment epithelium-derived factor mRNA and factor VIII-related antigen staining. We have observed previously that the highest VEGF levels among the Dunning tumors were found in the metastatic sublines (11). To study if there was a similar difference in the human prostate tumors, the VEGF mRNA levels were examined in the microdissected tumor epithelial cells. There was no significant difference in the VEGF mRNA levels between the M0 and M1 groups, and in line with the mRNA data, the immunohistochemical staining for VEGF showed no variation between the two patient groups (data not shown). To ensure that equal levels of RNA were analyzed in the M0 and M1 groups during the reverse transcription-PCR procedure, GAPDH mRNA levels were quantified. No significant difference in GAPDH mRNA levels between the groups was observed, and GAPDH did not correlate with either the vascular count or the proliferation index (results not shown). These data suggest that decreased pigment epithelium-derived factor expression may also be associated with a metastatic phenotype in human prostate cancers.

## DISCUSSION

Previous studies in human prostate cancer indicated that pigment epithelium-derived factor expression is lost in prostate cancer, and in mice, when pigment epithelium-derived factor was knocked out, proliferation index and vascular density increased in the prostate (31, 32). Together, these data suggest that decreased pigment epithelium-derived factor expression may contribute to tumor progression, possibly through increased tumor cell proliferation and increased angiogenesis. Here, we have shown in the Dunning rat model that pigment epithelium-derived factor is significantly higher in well-differentiated, nonmetastatic, androgen-sensitive tumors and in anaplastic and androgen-insensitive but nonmetastatic tumors compared with metastatic tumor sublines. The observation of decreased pigment epithelium-derived factor levels in metastatic rodent tumors prompted us to additionally examine the pigment epithelium-derived factor levels in poorly differentiated human prostate cancer in relation to metastases. Poorly differentiated prostate cancer (Gleason score 8–10) is usually a highly aggressive disease that rapidly forms metastases and kills the patient within a few years (35). Using a large historical series of transurethral resection diagnosed prostate cancers with long-term follow-up, we selected a subset of poorly differentiated prostate cancers that had a more favorable outcome with no bone metastases present at diagnosis and all of the patients surviving >7 years. These tumors were compared with the tumors from patients with the more common phenotype, *i.e.*, with the same local tumor stage and Gleason score, but with metastases at diagnosis and who died of prostate cancer within a few years. In striking similarity to the observations in the Dunning model, we found that the patients with the poorly differentiated tumors with more favorable outcome and low metastatic capacity had higher pigment epithelium-derived factor levels. These findings are consistent with published studies and indicate that decreased pigment epithelium-derived factor expression could be associated with the metastatic phenotype in prostate cancer. Interestingly, pigment epithelium-derived factor expression was inversely correlated to metastasis and outcome also in pancreas cancer (41). In pigment epithelium-derived factor knockout mice, prostate and pancreas size were increased, and this was associated with increased vascular density and epithelial cell hyperplasia (31). Pigment epithelium-derived factor apparently plays a particularly important role in angiogenesis, tissue growth, and metastasis in these two glands.

High pigment epithelium-derived factor levels could inhibit metastasis in several ways. For example, it could suppress angiogenesis, inhibit tumor cell proliferation, increase tumor cell apoptosis, and/or decrease tumor cell migration and invasiveness. We have observed previously that tumor VEGF synthesis and vascular density are gradually increased during tumor progression in Dunning tumors. The highest vascular density and VEGF levels were found in the metastatic sublines AT-3 and MatLyLu (11), and in this study we confirmed that vascular density is considerably higher in MatLyLu than in AT-1 tumors. The present observation that pigment epithelium-derived factor is low in the metastatic tumor subtypes and that the high VEGF levels are not counteracted by this inhibitor could explain why they have the highest vascular density. A putative pigment epithelium-derived factor receptor has been isolated from retinoblastoma tumor cells (42) and from normal neural retinal cells (43); however, nothing is known about possible endothelial or tumor cell pigment epithelium-derived factor receptors in the prostate. It could be possible, as well, that pigment epithelium-derived factor competes with, or inhibits, VEGF binding to its receptor. However, there is currently no data to support this. Tumor cell proliferation was also higher in MatLyLu than in AT-1 tumors. Thus, decreased pigment epithelium-derived factor is associated with increased angiogenesis, increased tumor cell proliferation, and also with a decreased tumor doubling time (34). It appears that the biological behavior in two anaplastic and morphologically rather similar prostate tumors is highly influenced by differences in the secretion of two factors, VEGF and pigment epithelium-derived factor, regulating the tumor vasculature. In resemblance, poorly differentiated, nonmetastatic human prostate tumors had a significantly higher pigment epithelium-derived factor:VEGF ratio, a lower tumor cell proliferation, and a low density of endoglin-stained blood vessels compared with poorly differentiated tumors with metastatic lesions at diagnosis. The density of factor VIII-related antigen stained vessels was, however, not significantly different. The reason for this is unknown, but endoglin is believed to be a better marker for ongoing angiogenesis than factor VIII-related antigen in prostate cancer (6). High pigment epithelium-derived factor levels were, however, more closely associated with decreased tumor cell proliferation than with vascular count in the human tumors. These data support our previous observation that pigment epithelium-derived factor has direct effects on tumor cells (31), and taken together it appears that high pigment epithelium-derived factor levels may render a less aggressive subset of poorly differentiated human prostate tumors.

Caspin, a murine homologue to pigment epithelium-derived factor, which binds specifically to collagen I and III in the extracellular matrix, is highly expressed in nonmetastatic colon cancer cell lines and low in metastatic variants demonstrating a relation among pigment epithelium-derived factor expression, metastasis, and cell adhesion (44). In line with this, overexpression of pigment epithelium-derived factor decreases the invasiveness of glioma cells *in vitro* (45). Interestingly, the reactive stroma formed during prostate tumor progression is characterized by a marked increase in collagen I synthesis and deposition around the tumor glands (46, 47). Maspin, another member of the serine protease inhibitor family, with collagen-binding characteristics very similar to pigment epithelium-derived factor (48, 49), is a well-known tumor suppressor in breast cancer (50–53) and has been shown recently to work as a tumor suppressor also in prostate cancer by increasing cell adhesion to the matrix (54). Therefore, it is possible that pigment epithelium-derived factor expression increases tumor cell adhesion to the surrounding matrix, and loss of

pigment epithelium-derived factor in prostate tumors may facilitate tumor cell migration and metastasis.

Because pigment epithelium-derived factor is know to have different functions in different cell types and under different conditions (55), it could have multiple roles in the prostate, *i.e.*, regulating the vasculature, epithelial cell proliferation, and migration. If pigment epithelium-derived factor does contribute to the metastatic capacity of poorly differentiated prostate cancer, it would be of interest to know why some tumors have higher levels than others. The previous study (31) has shown that pigment epithelium-derived factor synthesis in the prostate is suppressed by hypoxia and androgens. The distinct perivascular pigment epithelium-derived factor expression in the AT-1 tumors suggest that the tumor cells in the less vascularized and hypoxic parts of these tumors, adjacent to overt necrosis, are able to respond to this microenvironment by decreasing pigment epithelium-derived factor expression. The physiological hypoxic down-regulation of pigment epithelium-derived factor expression could thus be intact in AT-1 cells. MatLyLu tumors cells, in contrast, synthesize very little pigment epithelium-derived factor *in vivo* in the normoxic perivascular regions, suggesting dysregulation of pigment epithelium-derived factor synthesis in these tumors. The underlying mechanism of this dysregulation is unknown, but the observation of highly different pigment epithelium-derived factor levels in AT-1 and MatLyLu cells cultured *in vitro* under identical conditions may suggest inherent differences rather than simple loss of normal hypoxia response. The pigment epithelium-derived factor gene (*Serpinf1*) resides on human chromosome 17p13.3 (56), a region commonly demonstrating loss of heterozygosity in prostate cancers (57, 58). Such genetic deletion could be one mechanism by which pigment epithelium-derived factor is silenced in tumors, as has been shown for several metastasis suppressor genes (59).

Here, we have observed that pigment epithelium-derived factor expression is inversely correlated with metastasis in the Dunning rat prostate cancer model and also in poorly differentiated human prostate cancer. In addition, these data, and our previous study (31), suggest that pigment epithelium-derived factor has direct effects on prostate tumor cells. Together, these data strongly suggest that pigment epithelium-derived factor is a metastasis suppressor in the human prostate and therefore warrants additional examination.

## REFERENCES


1. Wakui S, Furusato M, Itoh T, et al. Tumour angiogenesis in prostatic carcinoma with and without bone marrow metastasis: a morphometric study. J Pathol 1992;168:257–62.
2. Brawer MK, Deering RE, Brown M, Preston SD, Bigler SA. Predictors of pathologic stage in prostatic carcinoma. The role of neovascularity. Cancer 1994;73:678–87.
3. McNeal JE, Yemoto CE. Significance of demonstrable vascular space invasion for the progression of prostatic adenocarcinoma. Am J Surg Pathol 1996;20:1351–60.
4. Furusato M, Wakui S, Sasaki H, Ito K, Ushigome S. Tumour angiogenesis in latent prostatic carcinoma. Br J Cancer 1994;70:1244–6.
5. Lissbrant IF, Stattin P, Damber JE, Bergh A. Vascular density is a predictor of cancer-specific survival in prostatic carcinoma. Prostate 1997;33:38–45.
6. Wikstrom P, Lissbrant IF, Stattin P, Egevad L, Bergh A. Endoglin (CD105) is expressed on immature blood vessels and is a marker for survival in prostate cancer. Prostate 2002;51:268–75.
7. Weidner N, Carroll PR, Flax J, Blumenfeld W, Folkman J. Tumor angiogenesis correlates with metastasis in invasive prostate carcinoma. Am J Pathol 1993;143:401–9.
8. Bouck N, Stellmach V, Hsu SC. How tumors become angiogenic. Adv Cancer Res 1996;69:135–74.
9. Hanahan D, Folkman J. Patterns and emerging mechanisms of the angiogenic switch during tumorigenesis. Cell 1996;86:353–64.
10. Lissbrant IF, Lissbrant E, Damber JE, Bergh A. Blood vessels are regulators of growth, diagnostic markers and therapeutic targets in prostate cancer. Scand J Urol Nephrol 2001;35:437–52.
11. Haggstrom S, Bergh A, Damber JE. Vascular endothelial growth factor content in metastasizing and nonmetastasizing Dunning prostatic adenocarcinoma. Prostate 2000;45:42–50.
12. Ferrer FA, Miller LJ, Andrawis RI, et al. Vascular endothelial growth factor (VEGF) expression in human prostate cancer: in situ and in vitro expression of VEGF by human prostate cancer cells. J Urol 1997;157:2329–33.
13. Harper ME, Glynne-Jones E, Goddard L, Thurston VJ, Griffiths K. Vascular endothelial growth factor (VEGF) expression in prostatic tumours and its relationship to neuroendocrine cells. Br J Cancer 1996;74:910–6.
14. Truong LD, Kadmon D, McCune BK, Flanders KC, Scardino PT, Thompson TC. Association of transforming growth factor-beta 1 with prostate cancer: an immunohistochemical study. Hum Pathol 1993;24:4–9.
15. Wikstrom P, Stattin P, Franck-Lissbrant I, Damber JE, Bergh A. Transforming growth factor beta1 is associated with angiogenesis, metastasis, and poor clinical outcome in prostate cancer. Prostate 1998;37:19–29.
16. Giri D, Ropiquet F, Ittmann M. Alterations in expression of basic fibroblast growth factor (FGF) 2 and its receptor FGFR-1 in human prostate cancer. Clin Cancer Res 1999;5:1063–71.
17. Ropiquet F, Giri D, Lamb DJ, Ittmann M. FGF7 and FGF2 are increased in benign prostatic hyperplasia and are associated with increased proliferation. J Urol 1999;162:595–9.
18. Ferrer FA, Miller LJ, Andrawis RI, et al. Angiogenesis and prostate cancer: in vivo and in vitro expression of angiogenesis factors by prostate cancer cells. Urology 1998;51:161–7.
19. Moore BB, Arenberg DA, Stoy K, et al. Distinct CXC chemokines mediate tumorigenicity of prostate cancer cells. Am J Pathol 1999;154:1503–12.
20. Mehta R, Kyshtoobayeva A, Kurosaki T, et al. Independent association of angiogenesis index with outcome in prostate cancer. Clin Cancer Res 2001;7:81–8.
21. Doll JA, Reiher FK, Crawford SE, Pins MR, Campbell SC, Bouck NP. Thrombospondin-1, vascular endothelial growth factor and fibroblast growth factor-2 are key functional regulators of angiogenesis in the prostate. Prostate 2001;49:293–305.
22. Jin RJ, Kwak C, Lee SG, et al. The application of an anti-angiogenic gene (thrombospondin-1) in the treatment of human prostate cancer xenografts. Cancer Gene Ther 2000;7:1537–42.
23. Dawson DW, Volpert OV, Gillis P, et al. Pigment epithelium-derived factor: a potent inhibitor of angiogenesis. Science 1999;285:245–8.
24. Stellmach V, Crawford SE, Zhou W, Bouck N. Prevention of ischemia-induced retinopathy by the natural ocular antiangiogenic agent pigment epithelium-derived factor. Proc Natl Acad Sci USA 2001;98:2593–7.
25. Tombran-Tink J, Chader GG, Johnson LV. PEDF: a pigment epithelium-derived factor with potent neuronal differentiative activity. Exp Eye Res 1991;53:411–4.
26. Taniwaki T, Becerra SP, Chader GJ, Schwartz JP. Pigment epithelium-derived factor is a survival factor for cerebellar granule cells in culture. J Neurochem 1995;64:2509–17.
27. Sugita Y, Becerra SP, Chader GJ, Schwartz JP. Pigment epithelium-derived factor (PEDF) has direct effects on the metabolism and proliferation of microglia and indirect effects on astrocytes. J Neurosci Res 1997;49:710–8.
28. Pignolo RJ, Cristofalo VJ, Rotenberg MO. Senescent WI-38 cells fail to express EPC-1, a gene induced in young cells upon entry into the G0 state. J Biol Chem 1993;268:8949–57.
29. Steele FR, Chader GJ, Johnson LV, Tombran-Tink J. Pigment epithelium-derived factor: neurotrophic activity and identification as a member of the serine protease inhibitor gene family. Proc Natl Acad Sci USA 1993;90:1526–30.
30. Becerra SP, Sagasti A, Spinella P, Notario V. Pigment epithelium-derived factor behaves like a noninhibitory serpin. Neurotrophic activity does not require the serpin reactive loop. J Biol Chem 1995;270:25992–9.
31. Doll JA, Stellmach VM, Bouck NP, et al. Pigment epithelium-derived factor regulates the vasculature and mass of the prostate and pancreas. Nat Med 2003;9:774–80.
32. Singh D, Febbo PG, Ross K, et al. Gene expression correlates of clinical prostate cancer behavior. Cancer Cell 2002;1:203–9.
33. Landstrom M, Damber JE, Bergh A, Tomic R, Carlsson-Bostedt L, Stigbrand T. Antiestrogens do not counteract the inhibitory effect of estradiol-17 beta on the growth of the Dunning R3327 prostatic adenocarcinoma. Prostate 1988;12:287–98.
34. Isaacs JT, Isaacs WB, Feitz WF, Scheres J. Establishment and characterization of seven Dunning rat prostatic cancer cell lines and their use in developing methods for predicting metastatic abilities of prostatic cancers. Prostate 1986;9:261–81.
35. Egevad L, Granfors T, Karlberg L, Bergh A, Stattin P. Prognostic value of the Gleason score in prostate cancer. BJU Int 2002;89:538–42.
36. Stattin P, Damber JE, Karlberg L, Bergh A. Cell proliferation assessed by Ki-67 immunoreactivity on formalin fixed tissues is a predictive factor for survival in prostate cancer. J Urol 1997;157:219–22.
37. UICC. TNM classification of malignant tumours 92. Berlin: Springer Verlag; 1992.
38. Stattin P, Westin P, Damber JE, Bergh A. Short-term cellular effects induced by castration therapy in relation to clinical outcome in prostate cancer. Br J Cancer 1998;77:670–5.
39. Lissbrant IF, Lissbrant E, Persson A, Damber JE, Bergh A. Endothelial cell proliferation in male reproductive organs of adult rat is high and regulated by testicular factors. Biol Reprod 2003;68:1107–11.
40. Specht K, Richter T, Muller U, Walch A, Werner M, Hofler H. Quantitative gene expression analysis in microdissected archival formalin-fixed and paraffin-embedded tumor tissue. Am J Pathol 2001;158:419–29.
41. Uehara H, Miyamoto M, Kato K, et al. Expression of pigment epithelium-derived factor decreases liver metastasis and correlates with favorable prognosis for patients with ductal pancreatic adenocarcinoma. Cancer Res 2004;64:3533–7.
42. Singh VK, Chader GJ, Rodriguez IR. Structural and comparative analysis of the mouse gene for pigment epithelium-derived factor (PEDF). Mol Vis 1998;4:7.

43. Alberdi E, Aymerich MS, Becerra SP. Binding of pigment epithelium-derived factor (PEDF) to retinoblastoma cells and cerebellar granule neurons. Evidence for a PEDF receptor. J Biol Chem 1999;274:31605–12.
44. Kozaki K, Miyaishi O, Koiwai O, et al. Isolation, purification, and characterization of a collagen-associated serpin, caspin, produced by murine colon adenocarcinoma cells. J Biol Chem 1998;273:15125–30.
45. Guan M, Pang CP, Yam HF, Cheung KF, Liu WW, Lu Y. Inhibition of glioma invasion by overexpression of pigment epithelium-derived factor. Cancer Gene Ther 2004;11:325–32.
46. Tuxhorn JA, Ayala GE, Rowley DR. Reactive stroma in prostate cancer progression. J Urol 2001;166:2472–83.
47. Tuxhorn JA, Ayala GE, Smith MJ, Smith VC, Dang TD, Rowley DR. Reactive stroma in human prostate cancer: induction of myofibroblast phenotype and extracellular matrix remodeling. Clin Cancer Res 2002;8:2912–23.
48. Blacque OE, Worrall DM. Evidence for a direct interaction between the tumor suppressor serpin, maspin, and types I and III collagen. J Biol Chem 2002;277:10783–8.
49. Meyer C, Notari L, Becerra SP. Mapping the type I collagen-binding site on pigment epithelium-derived factor. Implications for its antiangiogenic activity. J Biol Chem 2002;277:45400–7.
50. Zou Z, Anisowicz A, Hendrix MJ, et al. Maspin, a serpin with tumor-suppressing activity in human mammary epithelial cells. Science 1994;263:526–9.
51. Seftor RE, Seftor EA, Sheng S, Pemberton PA, Sager R, Hendrix MJ. Maspin suppresses the invasive phenotype of human breast carcinoma. Cancer Res 1998;58:5681–5.
52. Sheng S, Carey J, Seftor EA, Dias L, Hendrix MJ, Sager R. Maspin acts at the cell membrane to inhibit invasion and motility of mammary and prostatic cancer cells. Proc Natl Acad Sci USA 1996;93:11669–74.
53. Shi HY, Zhang W, Liang R, et al. Blocking tumor growth, invasion, and metastasis by maspin in a syngeneic breast cancer model. Cancer Res 2001;61:6945–51.
54. Abraham S, Zhang W, Greenberg N, Zhang M. Maspin functions as tumor suppressor by increasing cell adhesion to extracellular matrix in prostate tumor cells. J Urol 2003;169:1157–61.
55. Chader GJ. PEDF. Raising both hopes and questions in controlling angiogenesis. Proc Natl Acad Sci USA 2001;98:2122–4.
56. Goliath R, Tombran-Tink J, Rodriquez IR, Chader G, Ramesar R, Greenberg J. The gene for PEDF, a retinal growth factor is a prime candidate for retinitis pigmentosa and is tightly linked to the RP13 locus on chromosome 17p13.3. Mol Vis 1996;2:5.
57. Dumur CI, Dechsukhum C, Ware JL, et al. Genome-wide detection of LOH in prostate cancer using human SNP microarray technology. Genomics 2003;81:260–9.
58. Liberfarb MF, Lin M, Lechpammer M, et al. Genome-wide loss of heterozygosity from laser capture microdissected prostate cancer using single nucleotide allele (SNP) arrays and a novel bioinformatics platform dChipSNP. Cancer Res 2003;63:4781–5.
59. Jaeger EB, Samant RS, Rinker-Schaeffer CW. Metastasis suppression in prostate cancer. Cancer Metastasis Rev 2001;20:279–86.